Computers in Biology and Medicine 130 (2021) 104232

Contents lists available at ScienceDirect

Computers in Biology and Medicine

journal homepage: http://www.elsevier.com/locate/compbiomed

Assessing the feasibility of detecting epileptic seizures using non-cerebral sensor data

Alexandra Hamlin [a], Erik Kobylarz [b], James H. Lever [c], Susan Taylor [c], Laura Ray [a,*]

[a] Thayer School of Engineering, Dartmouth College, United States
[b] Geisel School of Medicine, Dartmouth College, Thayer School of Engineering, Dartmouth College (adjunct Appointment); and Dartmouth-Hitchcock Medical Center, United States
[c] Dartmouth College (adjunct Appointment) and U.S. Army ERDC, United States

ARTICLE INFO

Keywords:
Biomedical computing
Decision-support systems
Wearable sensors
Machine learning
Biomedical signal processing

ABSTRACT

This paper investigates the feasibility of using non-cerebral, time-series data to detect epileptic seizures. Data were recorded from fifteen patients (7 male, 5 female, 3 not noted, mean age 36.17 yrs), five of whom had a total of seven seizures. Patients were monitored in an inpatient setting using standard video-electroencephalography (vEEG), while also wearing sensors monitoring electrocardiography, electrodermal activity, electromyography, accelerometry, and audio signals (vocalizations). A systematic and detailed study was conducted to identify the sensors and the features derived from the non-cerebral sensors that contribute most significantly to separability of data acquired during seizures from non-seizure data. Post-processing of the data using linear discriminant analysis (LDA) shows that seizure data are strongly separable from non-seizure data based on features derived from the signals recorded. The mean area under the receiver operator characteristic (ROC) curve for each individual patient that experienced a seizure during data collection, calculated using LDA, was 0.9682. The features that contribute most significantly to seizure detection differ for each patient. The results show that a multimodal approach to seizure detection using the specified sensor suite is promising in detecting seizures with both sensitivity and specificity. Moreover, the study provides a means to quantify the contribution of each sensor and feature to separability. Development of a non-electroencephalography (EEG) based seizure detection device would give doctors a more accurate seizure count outside of the clinical setting, improving treatment and the quality of life of epilepsy patients.

1. Introduction

Around 65 million people worldwide have epilepsy, and about 3.4 million of these people live in the U.S [1,2]. Of people with epilepsy, 20–40% have refractory epilepsy, which means typical epilepsy medications do not control their seizures [3]. In order for doctors to prescribe the correct medication and gain an understanding of how epilepsy interferes with a patient's life, they rely on the patient's self-reported accounts of seizures. However, a study by Hoppe et al. [4] revealed that patients monitored in an Epilepsy Monitoring Unit (EMU) failed to report 55.5% of all seizures. When asked, 36 of the 91 patients (40%) believed they were fully aware of their seizures, yet their reporting showed that only 11 patients (12%) were able to accurately record all of their seizures. Experiments such as this have been reproduced with similar conclusions drawn [5,6].

Currently, the gold standard for seizure monitoring and detection is combined video and electroencephalography (vEEG) recording conducted in an EMU. While vEEG provides the most accurate results for seizure detection, it requires patients to wear numerous electrodes on their scalp (typically at least 25) and be continuously videotaped, making it unrealistic for everyday use. Furthermore, trained professionals need to review the EEG data to identify seizures. Consequently, a method is needed to accurately count seizures during day-to-day activity outside of a clinical setting.

Epileptic seizures can present a wide range of observable behaviors that relate to the nature of their onset and propagation within the brain. Table 1 provides brief descriptions of common seizure types. The observable changes in patient motion, vocalization, and physiological response during seizures offer non-cerebral signals that could be used to detect seizures. This paper presents a study whose aim is to determine

* Corresponding author.
E-mail address: lray@dartmouth.edu (L. Ray).

https://doi.org/10.1016/j.compbiomed.2021.104232
Received 6 September 2020; Received in revised form 13 January 2021; Accepted 17 January 2021
Available online 21 January 2021

Table 1
Common Seizure Types and their Manifestation.

Type	Manifestation
Tonic-Clonic	Muscle stiffening, jerking, shaking, loss of consciousness
Clonic	Rhythmic muscle spasms or jerking
Tonic	Muscle tensing
Myoclonic	Sudden muscle jerk as if shocked
Atonic	Loss of muscle tone
Absence (Petit Mal)	Blank staring, lack of responsiveness
Simple Focal	Change in smell or taste, extremity twitching, sweating
Complex Focal	Loss of consciousness, repetitive motions, e.g., lip smacking
Secondary Generalized	Muscle shaking or loss of tone

whether seizure activity of many types is separable from daily activities. Establishing separability is the first step towards developing a body-worn device for seizure detection using non-cerebral signals. Separating seizure behavior from long intervals of normal, non-seizure behavior is the key task of any detection scheme and is critical to avoiding frequent "nuisance" alarms from false detections. Hence separability is the central focus of this study.

To assess separability, we used linear discriminant analysis (LDA) on features derived from data recorded from inpatients via electrocardiography, electrodermal activity, electromyography, accelerometry, and audio signal monitoring. The results presented in this paper will guide the design of a self-contained device comprised of sensors and a real-time machine learning algorithm. The goal is a device that accurately detects and counts seizures occurring outside of the clinical setting with minimal interference on normal life. Establishing separability is the first step in the design process.

2. Prior research

Several research teams have investigated the use of accelerometers placed on or under mattresses to detect a patient's nocturnal seizures [7–10]. Other researchers have explored monitoring sleep through video and audio monitoring [11–14]. These studies have shown mixed results and are only useful for detecting convulsive seizures in a specific room.

Wearable devices have been studied to detect convulsive seizures specifically, which are associated with repeated, jerking motions of various parts of the body and are dissimilar to motions that occur during day-to-day life. The movements of convulsive seizures are observable in several signals such as accelerometry and electromyography (EMG).

In accelerometry signals, myoclonic, tonic clonic, and clonic seizures appear distinct from each other and from normal movements. A myoclonic seizure is characterized by muscle jerks that frequently occur in clusters [15]. At the end of a myoclonic seizure the patient goes limp and falls to the nearest surface, which manifests as a sudden spike in accelerometry data. During a tonic seizure, a person's body becomes rigid [16]. Tonic-clonic seizures are tonic seizures followed by clonic seizure, characterized by rapid jerking or shaking [17]. These seizure types appear distinct from each other and from normal movements in accelerometry data.

Nijsen et al. [18] monitored 18 patients with severe epilepsy for 36 h each and observed a total of 897 seizures through a combination of vEEG and accelerometry monitoring. The researchers report that 78% of seizures had a stereotypical tonic pattern, 74% a stereotypical myoclonic pattern, 14% a stereotypical clonic pattern, and 57% were preceded by a myoclonic seizure. Overall, they found that they were able to detect 48% of all seizures that occurred using accelerometry. Other studies have shown higher convulsive seizure detection rates using accelerometry alone [19–28]. Although accelerometry is useful for detecting convulsive seizures, it is not useful for detecting other types of seizures.

EMG, which measures muscle activation, is also used to detect convulsive seizures [21,29,30]. A myoclonic seizure, when a person's body falls limp upon conclusion of the seizure, would also be visible in EMG signals as all muscle activation would end suddenly. Like accelerometry, EMG is most useful in detecting convulsive seizures, but does not detect all seizure types.

To detect non-convulsive seizures, non-movement-based signals must be recorded using other sensors. During seizures, the autonomic nervous system is frequently activated, leading to variations in several biosignals. One of the most common changes during an epileptic seizure is an increase in heart rate due to the activation of the sympathetic nervous system [31–39]. Sinus tachycardia, or when the heart rate rises above 100 beats per minute, has been reported to occur in as many as 99% of seizures and frequently precedes the seizure onset by several seconds [34]. More importantly, potentially serious changes, such as ST-depressions and T-wave inversions in the electrocardiogram, were seen in 39% of seizures [37]. Heart rate variability also frequently increases during seizures, allowing researchers to differentiate between an increase in heart rate due to seizures and other daily activity such as exercise [38]. Still, ECG alone is not adequate for accurate seizure detection.

Activation of the autonomic nervous system during seizures also increases sweating, which can be detected through electrodermal (EDA) sensors [40]. However, people sweat for various reasons, so EDA is most useful when combined with other modalities. Thus, researchers have generally tested devices using EDA in conjunction with other sensors.

While many modalities are clearly useful in detecting seizures, none so far have been able to detect all types of seizures because of the wide variety of seizure manifestations. Several researchers have begun testing devices that use multiple modalities with mixed outcomes [41–46]. These studies relate most closely to the work presented in this paper.

Milošević et al. [41] reports results using accelerometry, but with added EMG sensors. They monitored 56 patients overnight, 7 of whom had a total of 22 seizures. Using a least-squares support vector machine (SVM), they were able to detect 91% of short and non-stereotypical seizures. Cogan et al. [42] presents a multimodal seizure detection system that uses a three-stage detection algorithm with photoplethysmography (PPG) to monitor heart rhythm, oxygen saturation measurements to observe breathing, and electrodermal activity (EDA) to evaluate sweating. Stage I quantifies signal activities, compares them to previous epochs of data, and looks specifically for an increase in heart rate followed by a decrease in oxygenation and then an increase in EDA consecutively. Stage II personalizes the algorithm by patient using pattern recognition and adjusting parameter levels. Stage III incorporates a limited suite of EEG channels into the detection. Cogan et al. [42] found that 100% of seizures were detected using Stages I and II alone from six of the ten patients who had seizures. Interestingly, Cogan et al. noted that their algorithm either detected all or none of an individual patient's seizures, so they assessed accuracy by patient rather than total seizure detection count. They were able to detect generalized tonic-clonic seizures more reliably than other seizure types, as expected, due to their more convulsive presentation. Finally, after incorporating three-channel EEG data into their analysis, Cogan et al. were able to detect 100% of seizures from eight of their ten patients [42]. Nonetheless, this would require placing electrodes on a patient's head during daily life, which is intrusive.

Becq et al. [43] used magnetic sensors and accelerometers on the arms and forehead to analyze 226 seizures in nine patients. Their goal was not to classify data as seizure or non-seizure, but to identify the type of seizure based on its motor manifestation. They artificially grew their dataset by duplicating each event 30 times and adding random noise. Then, they classified motor manifestation using an artificial neural network. This process resulted in 20% error between machine and standard vEEG analysis.

Poh et al. [44] used a Smartband [40,46] to record over 4000 h of data from 80 patients in an EMU. Though the Smartband includes more signals, they consider the accelerometry and EDA data in Ref. [44]. They analyze 10-s epochs of data using a 19-feature SVM. Their cross validation analysis considered both leave-one-patient-out and

Table 2
Summary of Patients monitored during study and Seizures Recorded.

Patient	Gender	Age	Length (h)	Seizures	Seizure Type
A[a]	F	42	21.01	0	N/A
B[a]	n.n	n.n	7.6	0	N/A
C[a]	n.n	n.n	19.87	0	N/A
D[a]	n.n	n.n	21.77	4	Complex partial, non-convulsive
E	M	51	44.88	0	N/A
F	M	21	4.44	0	N/A
G	F	36	19.43	0	N/A
H	F	36	21.03	0	N/A
I	M	41	75.85	2	Complex partial originating in the left temporal lobe
J	M	n.n	3.72	0	N/A
K	F	47	2.65	0	N/A
L	F	21	12.4	1	Psychogenic non-epileptic seizure (PNES)
A	F	42	37.31	2	Complex partial originating in the left temporal lobe
M	M	27	16.44	0	N/A
N	M	32	66.72	1	Partial originating in the left temporal lobe with secondary generalization, showed tonic clonic activity
O	M	58	7.67	1	Partial motor originating in the right frontal lobe with secondary generalization
TOTAL	7 M 5F	36.2	382.8	11	6 Complex Partial 2 Partial with Secondary Generalization 2 Partial Motor 1 Psychogenic Non-Epileptic

'n,n,' indicates that the information was not noted.
[a] Recorded with first system.

leave-one-seizure-out metrics. Overall, they detected 15 of 16 (94%) seizures. With this sensitivity, they also observed about one false positive per 24-h period, or a total of 28 false alarms. This gives a positive predictive value of 0.36.

Heldberg et al. [45] also studied the Smartband and also only considered EDA and accelerometry signals. Eight patients that had a total of 55 seizures over the 540 h of data recorded. The data were processed using 10 s windows with 50% overlap as well as 5-min windows with 80% overlap, then passed through a 1.5 Hz low-pass filter before extracting 26 features. A 10-tree random forest and kNN clustering with $k = 5$ algorithm were both tested. An overall sensitivity of 89.1% and a specificity of 93.1% were achieved. The precision was low at 7.5%, indicating a high rate of false positives. For predominantly non-motor seizures, they achieved a sensitivity of 97.1% with 9.6% precision and 92.9% specificity, also using kNN clustering. Overall, results from this study indicate that there is still a need for a more reliable seizure detection device.

While some methods are able to detect specific types of seizures, none are able to detect all types reliably. Generally, modalities that monitor movement, such as accelerometry and electromyography, are useful in identifying convulsive seizures. Other modalities, such as electro-cardiography and electrodermal activity, have proven to be useful in detecting non-convulsive seizures. Because some modalities are more useful in detecting specific types of seizures, combining many modalities should enable a larger range of seizure type detection. Thus, we hypothesize that combining several non-cerebral sensing modalities, and carefully choosing features that characterize the signals, will allow us to detect many seizure types. Moreover, a detailed study of separability of seizure and non-seizure activity will aid in identifying the most important sensors and features for seizure detection.

3. Methods

3.1. Dataset

The data for this study is recorded from fifteen patients in an epilepsy monitoring unit (EMU). Both male and female patients between ages 18 and 70 years old scheduled for admission to the Dartmouth-Hitchcock Medical Center EMU were screened for potential recruitment to the study. All patients or their legal guardians gave informed written consent following an Institutional Review Board protocol. Inclusion criteria were broad; both patients with poorly controlled seizures of partial (e.g., motor) onset that may or may not secondarily generalize, and patients experiencing primary generalized seizures (e.g., myoclonic and atypical absence with or without automatisms such as stereotypical facial and/or limb movements) were included in the study. The study called for patients who experience seizures on a relatively frequent basis to provide sufficient data for analysis. While being monitored, however, the majority of patients experienced no seizures, some experienced only one or two seizures and one patient experienced four seizures. Table 2 summarizes the main categories and manifestations of seizures experienced by each patient.

While in an EMU, patients are monitored using both EEG and video. In standard monitoring, doctors examine a patient's EEG and note when seizures occur. These seizures are then verified with the video record.

In this study, patients were simultaneously monitored with standard vEEG recording as well as with electrocardiograph (ECG), electromyography (EMG), electrodermal activity sensors (EDA), photoplethysmography (PPG), accelerometer (ACC), and a microphone. The vEEG data are used to hand-label the non-cerebral sensor data, i.e., to determine what patients were doing at different times, and to define the time of seizure onset and conclusion. To synchronize recording times with vEEG, a digital clock was placed in view of the EMU's video camera.

Data were collected over two separate time periods using different hardware. The original data set acquired for analysis by Azad et al. [47] used two Biopac MP36 data acquisition systems to collect patient data. One Biopac MP36 sampled the three accelerometer axes and a microphone at 50,000 Hz, while the other sampled ECG, EMG, and EDA signals at 5000 Hz. To protect patient privacy, the microphone recorded only the high portions of a 100 ms square wave using a 555 Timer circuit, i.e., these 50 ms snapshots of vocalizations prohibit recording and decoding of the patient's conversations.

The second system used a single Biopac MP160 data acquisition system to acquire patient data. The Biopac MP160 connects to Biopac amplifiers for EDA, EMG, ECG, and photoplethysmography (PPG), as well as a Biopac tri-axial accelerometer. A custom microphone circuit, recording only high portions of the microphone signal convolved with a 100 ms square wave was recorded using an analog channel on the MP160. The microphone is sampled at 10 kHz, while the rest of the signals are sampled at 2.5 kHz.

Recording ECG data requires three electrodes placed on the chest. EDA uses two electrodes placed on the inner wrist. EMG measurement requires three electrodes placed on the inner forearm, and the accelerometer is attached to the wrist as well. The microphone as well as the Biopac system were placed on patients' bedside tables. The MP160 connects to a computer running Biopac AcqKnowledge 5.0 software to record the incoming data. Overall, 382.79 h of data were collected from fifteen different patients (5 female, 7 male, 3 not noted) between February 2016 and 2018.

3.2. Sample data

Different types of seizures appear differently in the signals collected. Convulsive seizures are particularly visible in accelerometry and EMG signals. Both convulsive and non-convulsive seizures frequently present with increased heart rate and heart rate variability as well as an increase

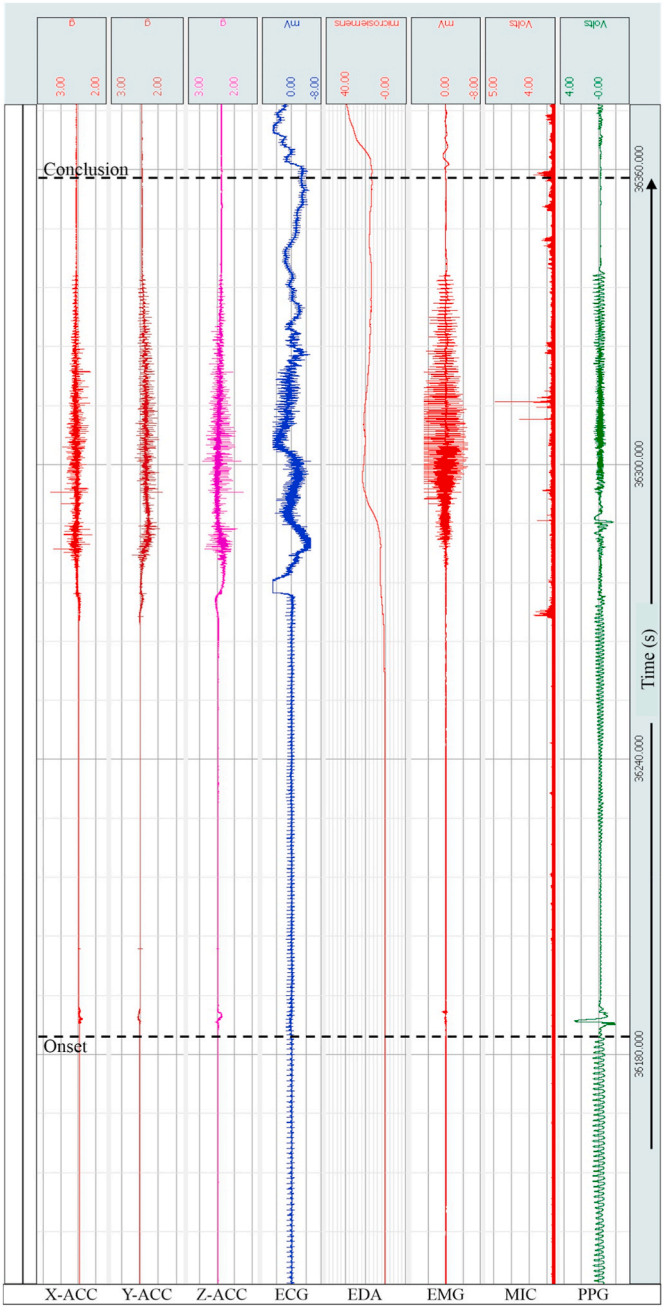

Fig. 1. Non-cerebral data for patient N's seizure. Signals are labeled below the waveforms: the first three signals from left to right show accelerometry, followed by ECG, EDA, EMG, MIC, which represents audio, and PPG signals on the y-axis and time on the x-axis. The seizure commenced at time 36,184 s and concluded at time 36,350 s. This figure shows a notable change in all signals during the patient's seizure.

in EDA. Aural automatisms may occur in either type of seizure and can be seen in audio signals. Thus, looking at the time-domain signals can provide insight into events during a seizure.

Fig. 1 plots the waveforms capturing patient N's seizure activity as an example of raw data manifestation of a seizure, including the 64 s immediately preceding the seizure and the 22 s following it. The seizure began at time 36,184 s and continued until time 36,350 s. The following account describes occurrences during the seizure, full annotations of which are documented in Table 3. Prior to the onset of the seizure, patient N was asleep. The start of the seizure is seen in the form of small blips in the accelerometer and EMG signals, as well as the sudden change

Table 3
Sample seizure data annotations.

Annotation	Time (sec)
Electrographic seizure onset, no clinical changes on video	36,184
Patient wakes up	36,188
Appears asleep again - might be moaning during this seizure	36,190
Right hand automatism, legs move under blanket.	36,231
Appears to sleep. Moaning?	36,235
Left head turning	36,269
Patient awake, vocalizes, picks up right arm	36,272
Right head turning	36,273
Whole body now rhythmically shaking	36,278
Automated seizure alarm	36,279
Less whole body shaking, RN at bedside	36,290
Whole body stiffened, back arched	36,296
RN: "Heart rate 92″	36,300
"Facial movements" patient rhythmic back jerking	36,305
Whole body rhythmic jerking slowing down, RN administers O2 mask	36,325
Patient twitching significantly less strong, has gagging sounds, not breathing	36,332
Now only left arm twitching	36,336
Minor back jerking x3	36,340
Gasping	36,342–36344
RN "Heart rate 101″	36,345
Seizure ends electrographically, per EEG reader	26,350
Patient takes deep breath	36,353
RN "69, heart rate 138" (I think that's what he says)	36,360
Deep breathing by patient	36,364
RN "Heart rate 124″	36,371
Deep breathing turns to snoring	36,420

in the PPG signal. Patient N woke up approximately 4 s into the seizure, and then appeared to be asleep again 2 s later. However, small changes were observed in the microphone signal during this time, indicating that the patient may have been moaning, but the video footage is unclear. At time 36,231 s (41 s into the seizure), N began having right hand automatisms and leg movement, although he appeared to be asleep. At time 36,272 s (88 s into the seizure), N woke up, vocalized, picked up his right arm, and began rhythmically turning his head. This change in behavior, marked by the first significant spike of the microphone signal, corresponds with the sudden dramatic change in the ECG signal as well as the fluctuations in the accelerometers. Six seconds later, N's whole body was observed to rhythmically shake, and the accelerometry and EMG signals both increased in magnitude. Approximately 12 s later the rhythmic shaking gradually abated. At time 36,296 s, N's whole body became rigid. Nine seconds later, N's back began jerking, evolving into a whole body rhythmical shake, leading to another increase in the magnitude of both the EMG and the accelerometry signals. At time 36,332 s, N's twitching lessened significantly and he produced gagging sounds, reflected by the microphone signal's increased magnitude. Four seconds later, only N's left arm was twitching. Finally, patient N gasped for 3 s, and at time 36,350 s, the seizure ended electrographically.

3.3. Filtering

While one may be able to visibly identify the difference between seizure and non-seizure time-series data, this difference needs to be defined by measurable properties to be automatically detected. To develop machine learning classifiers, properties of the waveforms are defined as features, and these features are extracted (i.e., calculated) from the time-series data. Prior to extracting features, the raw data are processed to reduce noise. For processing, data are segmented into 5-s increments or epochs, with each epoch overlapping the preceding epoch by 2.5 s (50%).

The Biopac ECG amplifier contains a built-in 0.005 Hz high pass filter and 150 Hz low pass filter. In Matlab, a forward-backward infinite impulse response (IIR) notch filter removes 60 Hz powerline noise and its harmonics which compromise the signal's integrity. The EMG signal is

Table 4
Features extracted from time series data.

Sensor	Feature Name	Feature Description
ECG	Avg. R-R Length	The average interval between R-waves
	Standard Deviation of the R-R Length	The standard deviation of the interval between R-waves
EMG	Mean Absolute Value	The average of the absolute value of the signal, $MeanAbs = mean\ (|x|)$
	Variance	The variance of the signal
	RMS	Root mean square value of the signal
	Waveform Length	Sum of the absolute value of the difference between N adjacent data points, $n = 1..N, WL = \sum |x_{n+1} - x_n|$
	Maximum	The maximum value of the signal
	Time High	Percent of data points above 75% of the signal's maximum
	Mean Fourier Transform	Average Fourier transform, $AvgFT = mean\ (fft(x))$
	Spectral Centroid	Center of mass of the EMG frequency spectrum
EDA	Maximum	The maximum of the signal
	Minimum	The minimum of the signal
	Average	The average of the signal
	Standard Deviation	The standard deviation of the signal
	Maximum Derivative	The maximum derivative of the signal, $MaxDeriv = \max\ (|diff(x)|)$
	Waveform Length	Sum of the absolute value of the difference between N adjacent data points, $n = 1..N, WL = \sum |x_{n+1} - x_n|$
	Spectral Centroid	Center of mass of the EDA frequency spectrum
Accelerometry	Average Magnitude	Average of the square root of the sum of squares of each axis, $AvgMag = mean\ ((x^2 + y^2 + y^2)^{1/2})$
	Standard Deviation	Standard deviation of the magnitude, $STDV = std\ ((x^2 + y^2 + y^2)^{1/2}$
	Maximum Magnitude	$MaxMag = \max\ ((x^2 + y^2 + y^2)^{1/2}$
	Average Fourier Transform	The average of the Fourier transform of the magnitude. $AvgFT = mean\ (fft\ ((x^2 + y^2 + y^2)^{1/2}$
	Average XY Correlation	The average of the correlation between the x and y axes, $AvgXYCorr = mean\ (corr\ (x,y))$
	Average XZ Correlation	The average of the correlation between the x and z axes, $AvgXZCorr = mean\ (corr\ (x,z))$
	Average YZ Correlation	The average of the correlation between the y and z axes, $AvgYZCorr = mean\ (corr\ (y,z))$
	Std. Dev. of XY Correlation	The standard deviation of the correlation between the x & y axes, $StdvXYCorr = std\ (corr\ (x,y))$
	Std. Dev. of XZ Correlation	The standard deviation of the correlation between the x & z axes, $StdvXZCorr = std\ (corr\ (x,z))$
	Std. Dev. of YZ Correlation	The standard deviation of the correlation between the y & z axes $StdvYZCorr = std\ (corr\ (y,z))$
	Spectral Centroid	Center of mass of the acceleration magnitude frequency spectrum
Microphone	Avg. Magnitude	The average magnitude of the signal
	Standard Deviation	The standard deviation of the signal
	Average Pitch	The average Fourier transform of the signal, $Pitch = mean\ (fft(x))$
	Spectral Centroid	Center of mass of the microphone frequency spectrum
	Bronchial Secretion Index	The sum of the Fourier transform between 2.2 and 2.6 Hz
	Linear Prediction Coefficient	The linear prediction coefficient of the signal using N = 2, $LPC = lpc\ (x,2)$

filtered using the Biopac EMG amplifier's built-in bandpass filter with 1 Hz high pass corner frequency and 500 Hz low pass corner frequency. Notch filtering in Matlab removes powerline noise in the same way as with ECG data. EDA signals have a bandwidth below 3 Hz. There is always some DC component to the signal because skin has a baseline conductance, so, the Biopac amplifier's built-in 10 Hz low pass filter removes this baseline signal. A 40 Hz corner frequency low pass digital filter designed in Matlab removes noise higher than 10 Hz. Accelerometry also includes a very low frequency component from gravity that shifts its distribution between the three axes as the patient moves. Thus, accelerometry and EDA are filtered in the same way. The same notch filtering used on ECG and EMG data also removes powerline noise in the microphone signal. The device records audio data convolved with a 100 ms square wave. We wrote Matlab code to remove the low periods of the square wave retaining only the positive 50 ms of the convolved signal to protect patient privacy, i.e., to assure that we were not recording patient conversations. PPG data are filtered with the Biopac built-in 0.05 Hz high pass filter and 10 Hz low pass filter.

3.4. Feature extraction and determination of separability

A review of the literature identified possible features to extract from filtered data [14,19,29,47,48]. From these studies, a broad range of features were selected so that their utility in differentiating between seizure and non-seizure data could be evaluated. The 34 features extracted are detailed in Table 4.

To evaluate the use of machine learning for detecting seizures from non-cerebral data we must first quantify the separability between seizure and non-seizure data, which is the primary purpose of this study. To do so, neurologists at the Dartmouth-Hitchcock Medical Center annotated vEEG data, labeling time segments of some of the data by what the patients were doing. Features were extracted from epochs of seizure and non-seizure data, and separability was evaluated using discriminant analysis.

We chose to look at four normal activities to compare individually and collectively to seizures – eating, sleeping, talking, and using technology (such as a typing on a phone or computer) using a binary classifier. We hypothesized that activities form clusters of data points as each has their own distinct signature in the various signals being recorded. Furthermore, we hypothesized that seizure activity is distinct from other daily activities allowing it to be detected. We explore the separability of seizure and non-seizure data using linear discriminant analysis (LDA) – a batch processing approach – before progressing to other approaches. LDA identifies a linear combination of features that separates two classes of data [49], in this case, seizure activity from the four normal activities. While LDA can be formulated as a non-binary classifier, in the result presented in Section 4, we only consider binary classification.

We implemented LDA on data for each individual patient as well as for multiple patients combined. LDA applied to data for an individual patient assesses the degree to which a linear decision boundary in multi-dimensional feature space (34 dimensions) separates seizure from non-seizure data for that individual, while applying LDA to data from multiple patients is a measure of whether a linear decision boundary can generalize. We use the area under the receiver operator characteristic (ROC) curve to quantify separability, where the ROC curve shows 1 – specificity or FP/(FP + TN) on the x-axis and sensitivity or TP/(TP + FN) on the y-axis. This study informs methods for training subsequent, recursive machine learning classifiers.

4. Results

Because the patients we monitored had seizures relatively infrequently, we recorded significantly more non-seizure data than seizure data. Thus, we selected varying set amounts of non-seizure data for analysis. If N represents the number of epochs we recorded from a patient during a seizure, we carried out analyses with N, Nx2, Nx5, Nx10 non-seizure epochs, as well as with all non-seizure data for that patient. N varies patient-to-patient as the number and length of seizures varies. Each analysis that does not include the full set of non-seizure data was executed 10,000 times, selecting a new random set of epochs within the

Table 5
Area under ROC mean and standard deviations by patient and non-seizure epochs used.

Patient	*N* Seizure Epochs, *N* Non-Seizure Epochs	*N* Seizure Epochs, *Nx2* Non-Seizure Epochs	*N* Seizure Epochs, *Nx5* Non-Seizure Epochs	*N* Seizure Epochs, *Nx10* Non-Seizure Epochs	*N* Seizure Epochs, All Non-Seizure Epochs
A	0.957 ± 0.0112	0.95806 ± 0.00821	0.96140 ± 0.00508	0.96480 ± 0.00354	0.9695
D	0.9381 ± 0.0292	0.93475 ± 0.02096	0.94022 ± 0.01268	0.94588 ± 0.00856	0.9549
I	0.9615 ± 0.0251	0.95125 ± 0.01924	0.94322 ± 0.01365	0.94063 ± 0.00975	0.938
N	0.9793 ± 0.0095	0.97825 ± 0.00661	0.97922 ± 0.00379	0.98072 ± 0.00251	0.9785
O	0.9998 ± 8.59E-04	0.99962 ± 0.00115	0.99973 ± 0.00059	0.99991 ± 0.00016	1

Table 6
Number of seizure epochs collected for each patient.

Patient	Number of Seizure Epochs by Patient, *N*
A	82
D	24
I	30
N	32
O	26

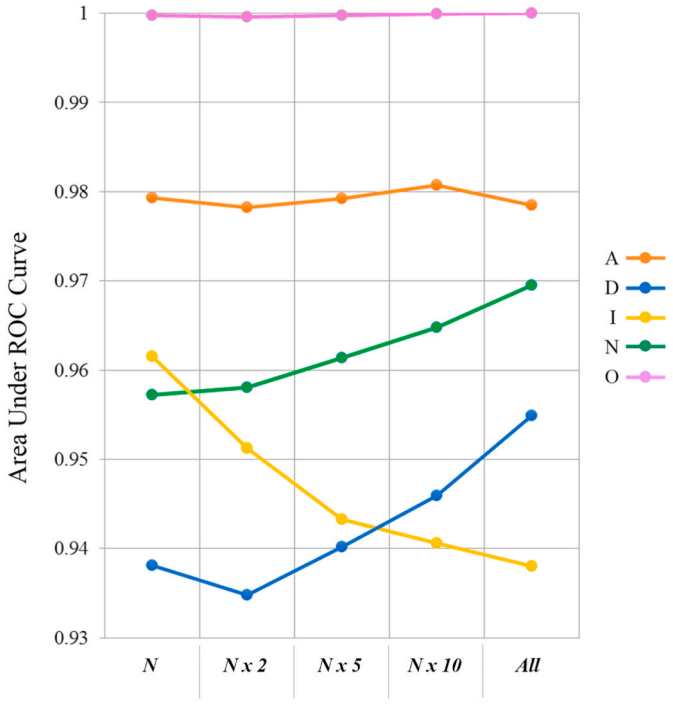

Fig. 2. Area under the ROC curve for individual patients as a function of *N*, or the number of non-seizure epochs that were included in analysis. This shows that the area under the ROC curve does not depend strongly on the amount of non-seizure data used.

non-seizure data for each iteration. This selection was conducted in order to ensure a representative sample set. For creating figures shown in this section, all 34 features described in Section 3 are used in LDA analysis.

The means and standard deviations over 10,000 trials for each set of analyses for individual patients are reported in Table 5. *N* is used in the title of each column as a variable representing the number of seizure epochs recorded, which varies by patient and is provided in Table 6. No standard deviation is reported when all non-seizure data are used as there is no variation when this analysis is repeated. Generally, values greater than 0.95 are considered good.

Fig. 2 shows a plot of the means in Table 6 for the five patients who experienced at least one seizure. The datapoint "All" denotes that all available non-seizure epochs were used to calculate the ROC for each patient. While values vary slightly based on how much non-seizure data are included, all values are greater than 0.9. It is interesting to note that while the curves for other patients either increase or remain relatively constant, the area under the ROC curve for patient I decreases as more non-seizure data are included. One possible explanation for this is that during his seizures, patient I simply stared ahead and was unresponsive; these behaviors are less distinct from non-seizure behaviors. As more non-seizure data are added, the presence of false positives and true negatives increases. By the same logic, the presence of true positives remains constant as no more seizure data are being added. Still, when all seizure and non-seizure data are included, the area under the ROC curve is 0.938 for patient I. In addition, patient D's seizures were also non-movement based and achieved an area under the ROC curve of 0.9549, demonstrating that non-movement seizures are separable from normal behavior.

Fig. 3 shows the histograms for visualization of separability derived from LDA analysis and provides the area under the ROC curves in the title for each patient that had at least one epileptic seizure, as well as for all five patients who had seizures combined. Each subfigure provides a normalized distance from the axis of maximal separation (AMS) on the horizontal axis vs. the frequency of occurrence of epochs within the seizure and non-seizure data. Plots 1 through 5 in Fig. 3 use the same number of seizure and non-seizure epochs for each individual patient, and plot 6 uses all seizure and non-seizure data from the five patients who experienced seizures.

All observations from the data support the same conclusion: while there is some overlap, seizure and non-seizure data are separable using the sensor suite and features described in section 3. We calculated the separation between the seizure data of all patients combined and all of the non-seizure data of all of the patients to explore how data from various patients generalize to others. The analysis presented uses all of the seizure data and all epochs of non-seizure data, and the area under the ROC curve is 0.9144. The area under this ROC curve is lower than for each individual patient. We hypothesize that one reason for this lower value is because we are including different types of seizures in the analysis. When more seizure data are available, classifiers can be tested on multiple occurrences of the same type of seizure to determine if they need to be patient-specific or not.

When using LDA, the separation between datasets is quantified by the magnitude of features along the AMS. Ranking features in order of their contribution to the AMS gives a metric of how useful they are in classifying activities. Thus, we can assess which features provide the most information by patient. Table 7 lists the first 10 features by importance for each patient. Table 7 also shows a combined feature set that was created by normalizing the means of each feature for each patient individually, taking the average for each feature across patients, and then re-sorting by magnitude to determine which features were overall the most important. To differentiate which features come from which sensors, the features are color-coded. Green represents a microphone feature, orange an EMG feature, blue an EDA feature, red an ECG feature, and purple represents an accelerometry feature. This shows that the most valuable sensors do vary by patient, even when patients experience similar seizure types. For example, the ten most important features for detecting the non-convulsive seizures of patients D and I share two common features, while convulsive patients N and O share three of the 10 most important features. EMG, microphone, EDA, and accelerometry features generally appear higher on the list than ECG features. Collecting more data and evaluating feature rank for additional patients and seizure types will provide further insight into which, if any,

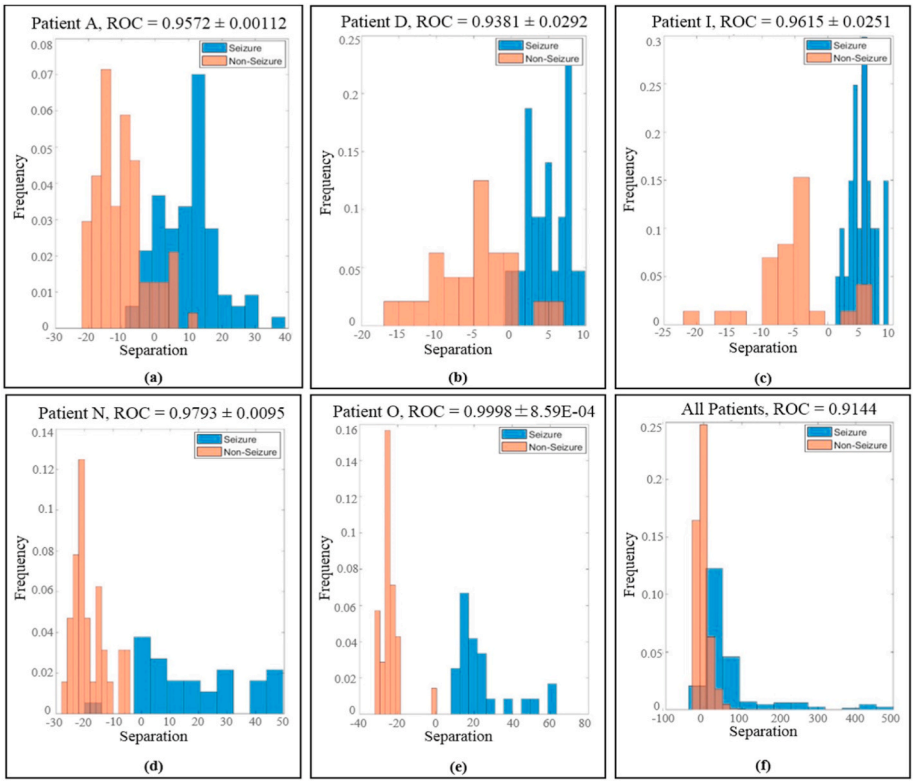

Fig. 3. Histograms showing separation of seizure and non-seizure epochs for each patient (a–e) and for all patients (f). Each count is an epoch, and separation values are the normalized value of the distance from the axis of maximal separation in 34-dimensional feature space.

Table 7
Ranking of most significant features for each patient and for all patients combined.

	D	N	A	I	O	Overall
1	EDA, Signal Length	MIC, Bronchial Secretion Index	MIC, Std. Dev.	EMG, Max	EDA, Max	MIC, Std. Dev.
2	MIC, Average Magnitude	MIC, Pitch	MIC, Bronchial Secretion Index	EMG, RMS	EDA, Average Magnitude	EMG, Mean Absolute Value
3	MIC, Std. Dev.	MIC, Spectral Centroid	MIC, Spectral Centroid	EMG, Mean Absolute Value	EDA, Min	EMG, RMS
4	ECG, Average Heartrate	EMG, Mean Absolute Value	EMG, Mean Absolute Value	EMG, Variance	EMG, Waveform Length	EMG, Max
5	ACC, Std. Dev.	EMG, Waveform Length	MIC, Pitch	EMG, Waveform Length	EDA, Spectral Centroid	EMG, Waveform Length
6	ACC, Max	EMG, RMS	EMG, RMS	MIC, Std. Dev.	EDA, Max Derivative	ACC, Average Magnitude
7	ACC, X-Y Corr. Std. Dev.	ACC, Average X-Y Corr.	EMG, Max	ACC, Std. Dev.	EMG, Mean Absolute Value	EMG, Variance
8	EDA, Min	ACC, Average X-Z Corr.	ACC, Std. Dev.	MIC, Spectral Centroid	EMG, RMS	ECG, Average Heartrate
9	EDA, Average Magnitude	EMG, Average Fourier Transform	ACC, Average Fourier Transform	MIC, Bronchial Secretion Index	EMG, Max	EDA, Min
10	EDA, Max	ACC, Max	EMG, Average Fourier Transform	MIC, Pitch	EDA, Std. Dev.	EDA, Average Magnitude

Color code: Pink – accelerometer; Green: EMG; Blue: EDA; Grey: Microphone; Orange: ECG.

Color code: Pink – accelerometer; Green: EMG; Blue: EDA; Grey: Microphone; Orange: ECG.

sensors and features can be eliminated.

Likewise, the analysis of separability using LDA sheds insight on and can be compared to the results previously reported for detection of seizures using a subset of the body-worn sensors considered here. For example, both Poh et al. [44] and Heldberg et al. [45] uses solely accelerometers and EDA to detect seizures. Poh et al. [44] reports detection of 15 out of 16 generalized tonic-clonic (motion) seizures from seven patients and a false alarm rate of 0.74 every 24 h. Heldberg et al.

Table 8
ROC values for individual sensors only, pairs of sensors compared to the full sensor suite.

	ACC only	MIC only	EDA only	EMG only	ECG only	ACC+EDA	ACC+MIC	Full sensor suite
A	0.7054	0.9655	0.2999	0.9218	0.3588	0.7112	0.9430	0.9695
D	0.7782	0.8976	0.5167	0.6182	0.1406	0.5844	0.8670	0.9549
I	0.2149	0.8224	0.4581	0.1507	0.5718	0.3780	0.6273	0.9380
N	0.9187	0.9433	0.9198	0.9165	0.5137	0.9579	0.9602	0.9785
O	0.9495	0.6190	1.0000	0.9976	0.6763	0.9999	0.9354	1.0000
Overall	0.7913	0.8282	0.6435	0.8660	0.4031	0.8279	0.8431	0.9144

[45] includes results from both motion and non-motion seizures reporting a lower overall sensitivity of 89.1% relative to Poh et al. and overall specificity of 93.1% for eight patients and 21 separate motion seizures. The sensitivity and specificity for seizures with no motor activity were 97.1% and 92.9%, respectively over 34 seizures. Table 8 shows a heat-map coded ROC values for the five patients who experienced seizures from our study, with motion classified in Table 2, and both single sensors and combinations of two sensors. These results are presented alongside the ROC for the full suite of sensors. These results show that no single sensor is adequate for seizure detection. Additionally, while for some patients (patients N and O) accelerometry combined with EDA provides ROC values over 0.95, for others, ROC value for these two sensors is unacceptably low. If only two sensors could be chosen for a device, Table 7 shows that accelerometry and microphone provide a ROC value above 0.86 for all but one patient. The full sensor suite retains ROC values above 0.93 for all patients individually, with an overall value on 0.9144.

5. Conclusion

Epilepsy is one of the most common neurological disorders, and accurate seizure tracking is crucial for effective epilepsy treatment. Currently, patients are expected to keep accurate records of their seizures. However, the majority of patients do not remember their seizures. Thus, a device to detect and track seizures is necessary. While some devices have shown positive results for specific types of seizures, none have been able to accurately detect all types. This work serves to improve seizure detection by combining modalities and systematically investigating separability of seizures from normal activity as a first step in developing a device that can detect all types of seizures.

We use electrocardiography, electrodermal activity, electromyography, accelerometry, and audio signals. Using linear discriminant analysis, we establish that seizure and non-seizure data from this sensor set are separable. When using all seizure and non-seizure data, the areas under the ROC curves for most patients are greater than 0.95, indicating strong separability. The area under the ROC curve for one patient is 0.938 Although the latter's seizures did not involve movement, another patient's seizures also did not include movement, but had an area under the ROC curve of 0.9549, suggesting that non-movement seizures are still separable from normal activity. Audio signal features, which are absent in other studies, prove to be among the top ten features establishing separability in four of five patients.

Strong separability of seizure and non-seizure data suggests that it should be possible to detect seizures in real time during normal routine. We moved towards real-time classification by implementing a support vector machine in Ref. [50]; preliminary results suggest that, with more data, a discriminative approach, such as a Support Vector Machine, may enable real-time classification, although additional data are needed [50].

Moving forward, we need to collect more patient data to develop multi-modal classifiers and to determine which features generalize across patients or across patients with similar seizure types and which features are specific to facilitating seizure detection in individual patients. With new data, various real-time machine learning classifiers can be explored. Overall, this research strongly suggests that non-cerebral sensing modalities provide data that can be accurately classified as seizure or non-seizure data using a discriminative machine learning method.

Declaration of competing interest

The authors have no conflicts of interests to declare.

Acknowledgements

This research was funded by the Hitchcock Foundation, a Reeves Pilot Project award and the Dept. of Defense Army Medical Research and Materiel Command, Award No. W81XWH18-1-0712.

References

[1] Institute of Medicine (US), Committee on the public health dimensions of the epilepsies, Washington D.C., in: M.J. England, C.T. Liverman, A.M. Schultz, L. M. Strawbridge (Eds.), "Introduction," in *Epilepsy Across the Spectrum, first* ed., National Academies Press (US), Washington D.C.), US, 2012, p. 27. ch. 1, sec. 2
[2] M.M. Zack, R. Kobau, "National and state estimates of the numbers of adults and children with active epilepsy – United States, 2015, Aug, 2017, MMWR Morb. Mortal. Wkly. Rep. 66 (31) (2017) 821–825, https://doi.org/10.15585/mmwr.mm6631a1 [Online].
[3] J.A. French, Refractory epilepsy: clinical overview, Epilepsia 48 (1) (Feb. 2007) 3–7, https://doi.org/10.1111/j.1528-1167.2007.00992.x [Online].
[4] C. Hoppe, A. Poepel, C. E. Elger, "Epilepsy: accuracy of patient seizure counts," Epilepsia, vol. 64, no. 11, pp. 1595-1599, DOI: 10.1001/archneur/64.11.1595, [Online].
[5] D. E. Blum, J. Eskola, J. J. Bortz, R. S. Fisher, "Patient awareness of seizures," Neurology, vol. 47, no. 1, 260-264, DOI: 10.1212/WNL.47.1.260, ([Online]).
[6] F. Kerling, S. Mueller, E. Pauli, H. Stefan, When do patients forget their seizures? An electroclinical study, Epilepsy Behav. 9 (2) (Sep. 2006) 281–285, https://doi.org/10.1016/j.yebeh.2006.05.050 ([Online]).
[7] A.P. Narechania, I.I. Garic, I. Sen-Gupta, M.P. Macken, E.E. Gerard, S.U. Schuele, Assesment of quasi-piezoelectric mattress monitor as a detection system for generalized convulsions, Epilepsy Behav. 28 (2) (Aug. 2013) 172–176, https://doi.org/10.1016/j.yebeh.2013.04.017 ([Online]).
[8] S. Fulton, K. Van Poppel, A. McGregor, M. Ellis, A. Patters, J. Wheless, Prospective study of 2 bed alarms for detection of nocturnal seizures, J. Child Neurol. 28 (11) (Oct. 2012) 1430–1433, https://doi.org/10.1177/0883073812462064 [Online].
[9] K. Van Poppel, S.P. Fulton, A. McGregor, M. Ellis, A. Patters, J. Wheless, Prospective study of the Emfit movement monitor, J. Child Neurol. 11 (11) (Jan. 2013) 1434–1436, https://doi.org/10.1177/0883073812471858 [Online]. C. Carlson, V. Arnedo, M. Cahill, O. Devinsky, "Detecting nocturnal convulsions: efficacy of the MP5 monitor," Seizure, vol. 18, no. 3, pp. 225–227, Apr. 2009. DOI: 10.1016/j.seizure.2008.08.007, [Online].
[10] H. Lu, Y. Pan, B. Mandal, H.L. Eng, C. Guan, D.W.S. Chan, Quantifying limb movements in epileptic seizures through color-based video analysis, IEEE Trans. Biomed. Eng. 60 (2) (Nov. 2012) 461–469, https://doi.org/10.1109/TBME.2012.2228649 ([Online]).
[11] S. Kalitzin, G. Petkov, D. Velis, B. Vledder, F. Lopes da Silva, Automatic segmentation of episodes containing epileptic clonic seizures in video sequences, IEEE Trans. Biomed. Eng. 59 (12) (Aug. 2012) 3379–3385, https://doi.org/10.1109/TBME.2012.2215609 [Online].
[12] L.L.C. Hipass Design, Sami: the sleep activity monitor [Online]. Available: www.samialert.com/details.
[13] G.R. de Bruijne, P.C.W. Sommen, R.M. Aarts, Detection of epileptic seizures through audio classification, in: 4th European Conf. Of the Int. Fed. For Med. And Biomed. Eng., Antwerp, Switzerland, 2008, pp. 23–27.
[14] Epilepsy Foundation, Myclonic seizures [Online]. Available: www.epilepsy.com/learn/types-seizures/myoclonic-seizures.
[15] Epilepsy Foundation, Tonic seizures [Online]. Available: www.epilepsy.com/learn/types-seizures/tonic-seizures.
[16] Epilepsy Foundation, Tonic-clonic seizures [Online]. Available, www.epilepsy.com/learn/types-seizures/tonic-clonic-seizures.

[17] T.M.E. Nijsen, R.M. Aarts, J.B.A.M. Arends, P.J.M. Cluitmans, Automated detection of tonic seizures using 3-D accelerometry, in: 4th European Conf. Of the Int. Fed. For Med. And Biomed. Eng., Antwerp, Switzerland, 2008, pp. 188–191.
[18] T.M.E. Nijsen, J.B.A.M. Arends, P.A.M. Griep, P.J.M. Cluitmans, The potential value of three-dimensional accelerometry for detection of motor seizures in severe epilepsy, Epilepsy Behav. 7 (1) (Aug. 2005) 74–84, https://doi.org/10.1016/j.yebeh.2005.04.011 [Online].
[19] S. Luca, P. Karsmakers, K. Cuppens, T. Croonenborghs, A. Van de Vel, B. Ceulemans, L. Lagae, S.V. Huffel, B. Vanrumste, Detecting rare events using extreme value statistics applied to epileptic convulsions in children, Artif. Intell. Med. 60 (2) (Feb. 2014) 89–96, https://doi.org/10.1016/j.artmed.2013.11007 [Online].
[20] A. Van de Vel, K. Cuppens, B. Bonroy, M. Milosevic, S. Van Huffel, B. Vanrumste, L. Lagae, B. Ceulemans, Long-term home monitoring of hypermotor seizures by patient-worn accelerometers, Epilepsy Behav. 26 (1) (Jan. 2013) 118–125, https://doi.org/10.1016/j.yebeh.2012.10.006 [Online].
[21] K. Cuppens, "reportDetection of Epileptic Seizures Based on Video and Accelerometer Readings," Ph.D. dissertation, E. E., Katholieke Univ. Leuven., Leuven, Belgium.
[22] G.T. Borujeny, M. Yazdi, A. Keshavarz-Haddad, A.R. Borujeny, Detection of epileptic seizure using wireless sensor networks, J. Med. Signals and Sens. 3 (2) (Apr. 2013) 63–68 ([Online]).
[23] A. Dalton, S. Patel, A.R. Chowdhury, M. Welsh, T. Pang, S. Schachter, G. OLaighin, P. Bonato, Development of a body sensor network to detect motor patterns of epileptic seizures, IEEE Trans. Biomed. Eng. 59 (11) (June 2012) 3204–3211, https://doi.org/10.1109/TBME.2012.2204990 [Online].
[24] J. Lockman, R.S. Fisher, D.M. Olson, Detection of seizure-like movements using a wrist accelerometer, Epilepsy Behav. 20 (4) (Apr. 2011) 638–641, https://doi.org/10.1016/j.yebeh.2011.01.019 ([Online]).
[25] A.L. Patterson, B. Mudigoudar, S. Fulton, A. McGregor, K. Van Poppel, M. C. Wheless, L. Brooks, J.W. Wheless, SmartWatch by SmartMonitor: assessment of seizure detection efficacy for various seizure types in children, a large prospective single-center study, Pediatr. Neurol. 53 (4) (Oct. 2015) 309–311, https://doi.org/10.1016/j.pediatrneurol.2015.07.002 [Online].
[26] S. Beniczky, T. Polster, T.W. Kjaer, W. Hjalgrim, Detection of generalized tonic-clonic seizures by a wireless wrist accelerometer: a prospective, multicenter study, Epilepsia 54 (4) (Apr. 2013), https://doi.org/10.1111/epi.12120 [Online].
[27] U. Kramer, S. Kipervasser, A. Schlitner, R. Kuzniecky, A novel portable seizure detection alarm system: preliminary results, J. Clin. Neurophysiol. 28 (1) (Feb. 2011) 36–38, https://doi.org/10.1097/WNP.0b013e3182051320 [Online].
[28] I. Conradsen, P. Wolf, T. Sams, H.B.D. Sorensen, S. Beniczky, Patterns of muscle activation during generalized tonic and tonic-clonic epileptic seizures, Epilepsia 52 (11) (Nov. 2011) 2125–2132, https://doi.org/10.1111/j.1528-1167.2011.03286.x [Online].
[29] I. Conradsen, S. Beniczky, K. Hoppe, P. Wolf, H.B.D. Sorensen, Automated algorithm for generalized tonic-clonic epileptic seizure onset detection based on sEMG zero-crossing rate, IEEE Trans. Biomed. Eng. 59 (2) (Dec. 2011) 579–585, https://doi.org/10.1109/TBME.2011.2178094 [Online].
[30] F. Leutmezer, C. Schernthaner, S. Lurger, K. Pötzelberger, C. Baumgartner, Electrocardiographic changes at the onset of epileptic seizures, Epilepsia 44 (3) (Mar. 2003) 348–354, https://doi.org/10.1046/j.1528-1157.2003.34702.x ([Online]).
[31] V. Novak, A. Reeves, P. Novak, P.A. Low, F.W. Sharbrough, Time-frequency mapping of R-R interval during complex partial seizures of temporal lobe origin, J. Auton. Nerv. Syst. 77 (2–3) (Sep. 1999) 195–202, https://doi.org/10.1016/S0165-1838(99)00044-2 ([Online]).
[32] I. Osorio, B.F. Manly, Is seizure detection based on EKG clinically relevant? Clin. Neurophysiol. 125 (10) (Oct. 2014) 1946–1951, https://doi.org/10.1016/j.clinph.2014.01.026 [Online].
[33] C. Opherk, J. Coromilas, L.J. Hirsch, Heart rate and EKG changes in 102 seizures: analysis of influencing factors, Epilepsy Res. 52 (2) (Dec. 2002) 117–127, https://doi.org/10.1016/S0920-1211(02)00215-2 [Online].
[34] C. Baumgartner, S. Lurger, F. Leutmezer, Autonomic symptoms during epileptic seizures, Epileptic Disord. 3 (3) (Sep. 2001) 103–116 [Online].
[35] O. Devinsky, Effects of seizures on autonomic and cardiovascular function, Epilepsy Current 4 (2) (Mar. 2004) 43–46, https://doi.org/10.1111/j.1535-7597.2004.42001.x [Online].
[36] M. Nei, R.T. Ho, M.R. Sperling, EKG abnormalities during partial seizures in refractory epilepsy, Epilepsia 41 (5) (May 2000) 542–548, https://doi.org/10.1111/j.1528-1157.2000.tb00207.x [Online].
[37] J. Jeppesen, S. Beniczky, P. Johansen, P. Sidenius, A. Fuglsang-Frederiksen, Detection of epileptic seizures with a modified heart rate variability algorithm based on Lorenz plot, Seizure 24 (Jan. 2015) 1–7, https://doi.org/10.1016/j.seizure.2014.11.004 [Online].
[38] I. Osorio, Automated seizure detection using EKG, Int. J. Neural Syst. 24 (2) (Mar. 2014) 1450001, https://doi.org/10.1142/S0129075614500014 [Online].
[39] W.J.C. van Elmpt, T.M.E. Nijsen, P.A.M. Griep, J.B.A.M. Arends, A model of heart rate changes to detect seizures in severe epilepsy, Seizure 15 (6) (Sep. 2006) 366–375, https://doi.org/10.1016/j.seizure.2006.03.005 [Online].
[40] M.Z. Poh, Continuous assessment of epileptic seizures with wrist-worn biosensors, Ph.D. dissertation, in: Harvard-MIT Div. Of Health Sci. and Tech., M.I.T., Cambridge, M.A., 2011.
[41] M. Milošević, A. Van de Vel, B. Bonroy, B. Ceulemans, L. Lagae, B. Vanrumste, S. Van Huffel, Automated detection of tonic-clonic seizures using 3-D accelerometry and surface electromyography in pediatric patients, J. Biomed. Health Inform. 20 (5) (Sep. 2016) 1333–1341, https://doi.org/10.1109/JBHI.2015.2462079 ([Online]).
[42] D. Cogan, J. Birjandtalab, M. Nourani, J. Harvey, V. Nagaraddi, Multi-biosignal analysis for epileptic seizure monitoring, Int. J. Neural Syst. 27 (1) (2017) 1650031, https://doi.org/10.1142/S0129065716500313 [Online].
[43] G. Becq, S. Bonnet, L. Minotti, M. Antonakios, R. Guillemaud, P. Kahane, Classification of epileptic motor manifestations using inertial and magnetic sensors, Comput. Biol. Med. 41 (1) (Jan. 2011) 46–55, https://doi.org/10.1016/j.compbiomed.2010.11.005 [Online].
[44] M.Z. Poh, T. Loddenkemper, C. Reinsberger, N.C. Swenson, S. Goyal, M.C. Sabtala, J.R. Madsen, R.W. Picard, Convulsive seizure detection using a wrist-worn electrodermal activity and accelerometry biosensor, Epilepsia 53 (5) (Mar. 2012) e93–e97, https://doi.org/10.1111/j.1528-1167.2012.0344.x ([Online]).
[45] B.E. Heldberg, T. Kautz, H. Leutheuser, R. Hopfengärtner, B.S. Kasper, B. M. Eskofier, Using wearable sensors for semiology-independent seizure detection –towards ambulatory monitoring of epilepsy, in: Presented at 37th Ann. Int. Conf. IEEE Eng. In Med. And Bio. Society, 2015, Aug.
[46] F. Oronati, G. Regalia, C. Caborni, M. Migliorini, D. Bender, M.Z. Poh, C. Frazier, E. Kovitch Thropp, E.E. Mynatt, J. Bidwell, R. Mai, W. C Jr., A.S. Blum, D. Friedman, T. Loddenkemper, F. Mohammadpour-Touserkani, C. Reinsberger, S. Tognetti, R.W. Picard, Multicenter clinical assessment of improved wearable multimodal convulsive seizure detectors, Epilepsia 58 (11) (Nov. 2017) 1870–1879, https://doi.org/10.1111/epi.13899 [Online].
[47] E. Azad, D. Bajpai, R. Butler, L. Sridhar, Final Design Review: A Device to Detect and Quantify Seizures, Thayer School of Engineering, Hanover, N.H., U.S., 2016.
[48] G.M. Azmal, A. Al-Jumaily, M. Al-Jaafreh, Continuous measurement of oxygen saturation level using photoplethysmography signal, in: Presented at Int. Conf. On Biom. And Pharm. Eng., 2006, 2007, Jan [Online]. Available: www.ieeeexplore.ieee.org/stamp/stamp.jsp?arnumber=4155955.
[49] S. Balakrishnama, A. Ganapathiraju, Linear discriminant analysis - a brief tutorial, Institute for Signal and information Processing 18 (1998). No. 1998.
[50] A. Hamlin, Epileptic Seizure Detection Using Multimodal Sensor Data and Machine Learning, Master of Science Thesis, Dartmouth College, 2019.